

Fig. S1. XRD pattern of AlO-NVO samples obtained by adjusting the ratio of Al to V (a) and $\text{NH}_4\text{V}_4\text{O}_{10-0}$ (b).

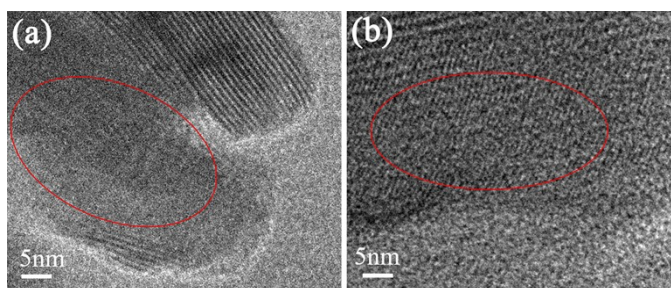


Fig. S2. HRTEM images of AlO-NVO-0.28.

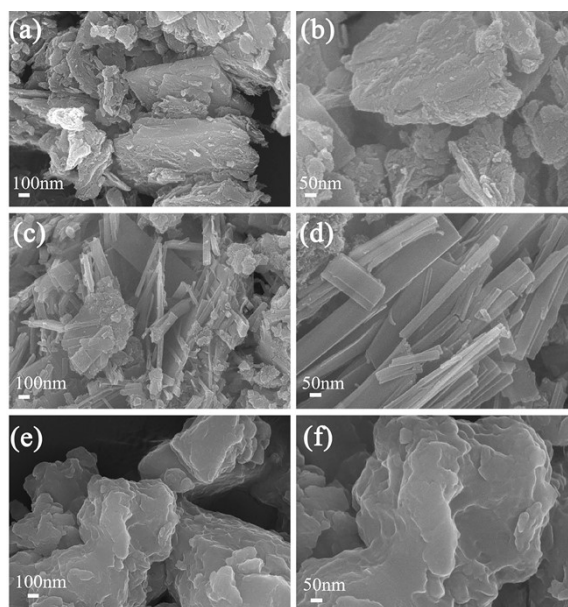


Fig. S3. The SEM images of AlO-NVO-0.56 (a-b), AlO-NVO-0.14 (c-d), and $\text{NH}_4\text{V}_4\text{O}_{10-0}$ (e-f).

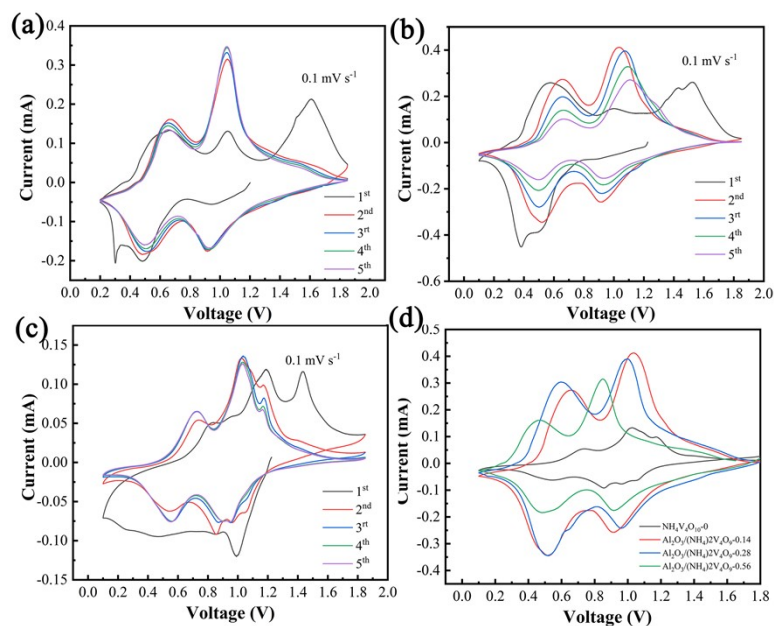


Fig. S4. The first five CV curves at the scan rate of 0.1 mV s^{-1} (a-c), the second and third CV curves (d) of AlO-NVO.0.28, AlO-NVO-0.14, AlO-NVO-0.56 and $\text{NH}_4\text{V}_4\text{O}_{10}\text{-0}$.

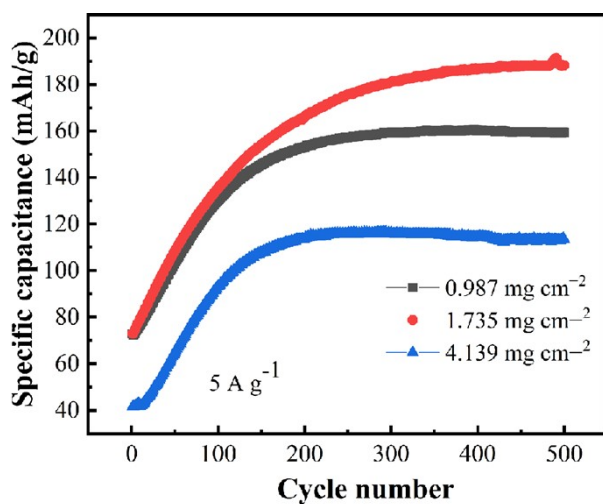


Fig. S5. The long-term cycling performance at the current density at 5.0 A g^{-1} of the AlO-NVO-0.28 with different load.

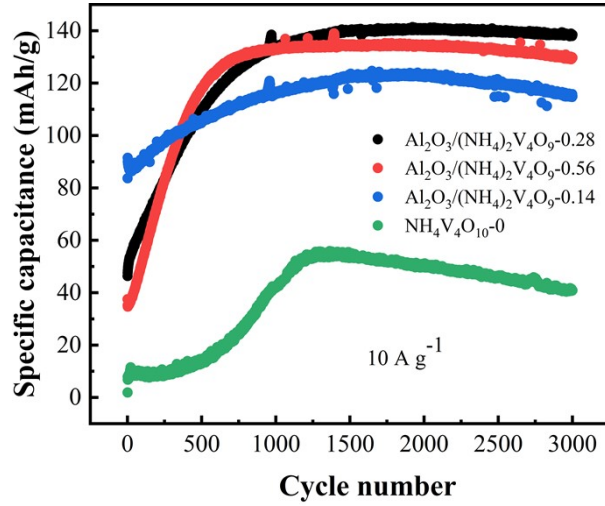


Fig. S6. The corresponding long-term cycling performance at the current density at 10.0 A g^{-1} of the AlO-NVO-0.28, AlO-NVO-0.14, AlO-NVO-0.56 and $\text{NH}_4\text{V}_4\text{O}_{10-0}$.

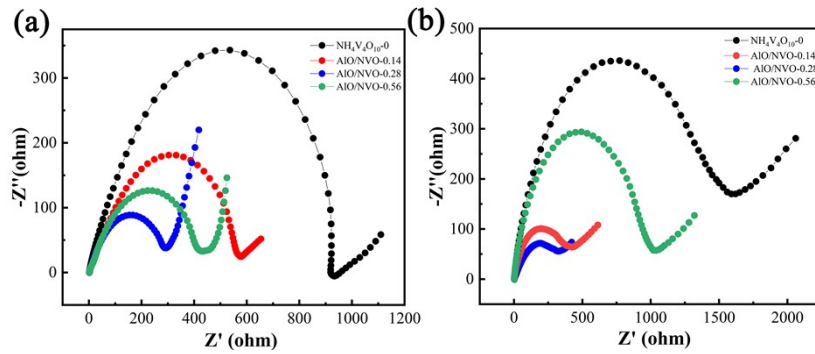


Fig. S7. Electrochemical impedance spectroscopy (EIS) patterns (a) initial state and (b) after 10 cycles of the four samples prepared by adjusting the amount of Al.

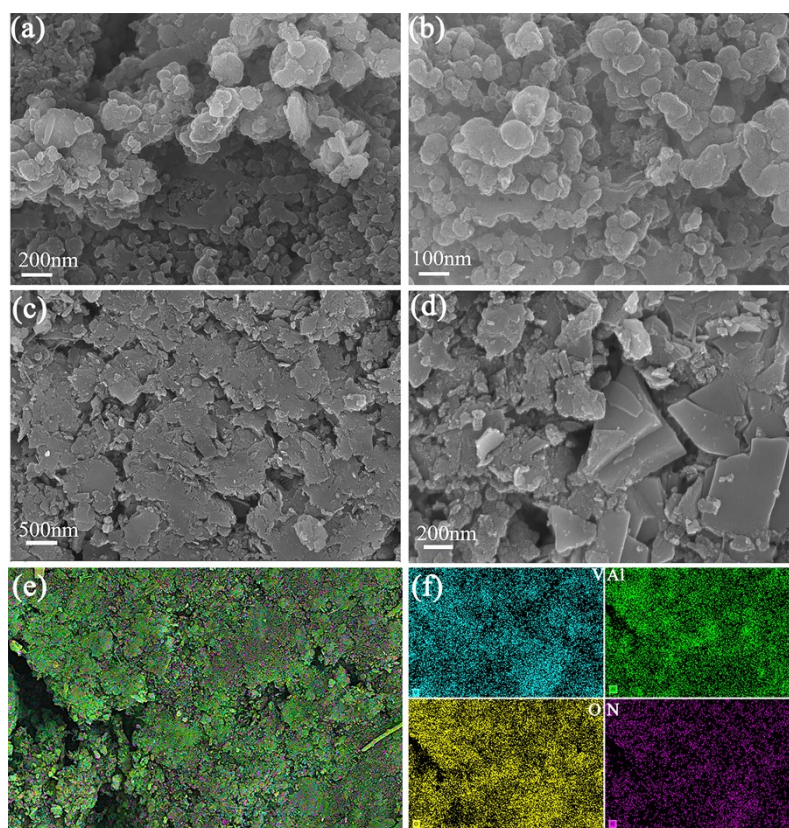


Fig. S8. The SEM images of the AlO-NVO-0.28 electrode after the 5 cycles (a-b), and their SEM images (c-d) EDS elemental mapping images (e-f) of the AlO/NVO-0.28 electrodes after the 500 cycles.

Table S1. Elemental analysis of Al and V in three AlO-NVO samples.

Sample name	Al: V(Actual dosage)	Al: V(ICP)	Al ₂ O ₃ proportion
AlO-NVO-0.56	0.56:1	0.52:1	21.49%
AlO-NVO-0.28	0.28:1	0.36:1	15.98%
AlO-NVO-0.14	0.14:1	0.16:1	8.01%

Table S2. Comparison of electrochemical properties of AlO-NVO with previously reported V-based cathode materials.

Materials	High discharge capacity	Capacity retention
Al ₂ O ₃ /(NH ₄) ₂ V ₄ O ₉	269 and 200 mAh g ⁻¹ at 0.5 and	86.5% after 3000

(this work)	5.0 A g ⁻¹ , respectively	cycles at 5.0 A g ⁻¹
(NH ₄) ₂ V ₆ O ₁₆ ·1.5H ₂ O [1]	284.6 and 172 mAh g ⁻¹ at 3.0 and 5.0 A g ⁻¹ , respectively	100% after 3000 cycles at 5.0 A g ⁻¹
(NH ₄) _x V ₂ O ₅ ·nH ₂ O [2]	372 and 219 mAh g ⁻¹ at 0.1 and 5.0 A g ⁻¹ , respectively	80% after 2000 cycles at 5.0 A g ⁻¹
(NH ₄) ₂ V ₄ O ₉ ·0.5H ₂ O [3]	200 and 177 mAh g ⁻¹ at 0.5 and 5.0 A g ⁻¹ , respectively	93% after 1000 cycles at 1.0 A g ⁻¹
NH ₄ V ₄ O ₁₀ [4]	355 and 280 mAh g ⁻¹ at 0.3 and 2.0 A g ⁻¹ , respectively	72% after 500 cycles at 3.0 A g ⁻¹
V ₂ O ₅ [5]	240 and 190 mAh g ⁻¹ at 0.029 and 0.147 mA g ⁻¹ , respectively	97% after 100 cycles at 0.15 A g ⁻¹
VS ₄ /CNTs [6]	265 and 182 mAh g ⁻¹ at 0.25 and 7 mA g ⁻¹ , respectively	93% after 1200 cycles at 5 A g ⁻¹
(NH ₄) ₂ Co ₂ V ₁₀ O ₂₈ ·16H ₂ O / (NH ₄) ₂ V ₁₀ O ₂₅ ·8H ₂ O [7]	367.7 and 238.7 mAh g ⁻¹ at 0.1 and 1.0 mA g ⁻¹ , respectively	82.1% after 1000 cycles at 1.0 A g ⁻¹
NH ₄ V ₃ O ₈ / Zn ₃ (OH) ₂ V ₂ O ₇ ·2H ₂ O [8]	332 and 132.6 mAh g ⁻¹ at 0.1 and 0.147 mA g ⁻¹ , respectively	92% after 1000 cycles at 10.0 A g ⁻¹

Reference:

- [1] X. Wang, B. Xi, Z. Feng, W. Chen, H. Li, Y. Jia, J. Feng, Y. Qian, S. Xiong, *J. Mater. Chem. A*, 2019, **7**, 19130–19139.
- [2] L. Xu, Y. Zhang, J. Zheng, H. Jiang, T. Hu, C. Meng, *Mater. Today Energy*, 2020, **18**, 100509.
- [3] R. Wei, X. Wang, B. Xi, Z. Feng, H. Li, W. Chen, Y. Jia, J. Feng, S. Xiong, *ACS Appl. Energy Mater.*, 2020, **3**, 5343–5352.
- [4] Y. Zheng, C. Tian, Y. Wu, L. Li, Y. Tao, L. Liang, G. Yu, J. Sun, S. Wu, F. Wang, Y. Pang, Z. Shen, Z. Pan, H. Chen, J. Wang, *Energy Storage Mater.*, 2022, **52**, 664–674

- [5] D. Batyrbekuly, B. Laïk, J.-P. Pereira-Ramos, Z. Bakenov, R. Baddour-Hadjean, *J. Energy Chem.*, 2021, **61**, 459–468.
- [6] S. Gao, P. Ju, Z. Liu, L. Zhai, W. Liu, X. Zhang, Y. Zhou, C. Dong, F. Jiang, J. Sun, *J. Energy Chem.*, 2022, **69**, 356–362.
- [7] W. Deng, Y. Xu, X. Zhang, C. Li, Y. Liu, K. Xiang, H. Chen, *J. Alloys Compd.*, 2022, **903**, 163824.
- [8] L. Liu , Z. Lin , Q. Shi, J. Tang , Z. Li , Z. Tao , W. Huang, *Electrochem. Comm.*, 2022, **140**, 107331.